Quantitative Study on a Multiscale Approach for OCT Retinal Layer Segmentation

A. González, C. Ortigueira, M. Ortega and M. G. Penedo
Department of Computer Science, University of A Coruña, A Coruña 15071, Spain

Keywords: OCT Retinal Images, Layer, Segmentation, Graph, Multiscale, Pyramidal.

Abstract: OCT technique for retinal imaging is establishing itself as a relevant modality among ophthalmologists due to its capacity to show more information than classical modalities. Nowadays, most image processing-based applications are emerging to extract that information automatically. As previous step of any automatic method to extract features from these images, the segmentation of the retinal layers has to be done. Graph-based methods provide good results for this problem, although their efficiency is an important limitation. In this work, a multiscale or pyramidal-based approach is studied in order to solve this problem. Different configurations are proposed to determine the optimal method. It is remarkable that this approach means an improvement not only in computation time, but also in segmentation results.

1 INTRODUCTION

Optical Coherence Tomography (OCT) images from the retina are used by experts to diagnose diseases, since their capture consists in a contact-less, non-invasive method that gives a cross sectional image of the retina in a real time fashion(Puzyeyeva et al., 2011). OCT provides information of the morphology in the retina in an effective way and it is useful to explain disease pathogenesis and heralding disease progression. In the recent years OCT has progressed, being the Spectral-domain (SD) OCT the current technique that ophthalmology experts use in their clinical practice because of its extremely high sensitivity and image-acquisition speed.

Several diseases can be diagnosed analyzing the OCT retinal images, some of them associated to human eye, such as glaucoma(Bowd et al., 2000), macular degeneration (Keane et al., 2012) and diabetic retinopathy(Sánchez-Tocino et al., 2002); but also diseases like multiple sclerosis(Albrecht et al., 2012), whose presence is strongly correlated with high-speed retinal thinning. In fact, several pathologies affect to the retinal layer morphology, so its appropriate segmentation is essential as a previous step in any diagnosing process.

The problem of the retinal layers segmentation has been studied using different approaches. One of the most effectives methods is that proposed in (Haeker et al., 2007), where the segmentation task is transformed into that of finding the minimum-closed-set in a geometric graph. Even though dynamic programming is proposed in (Chiu et al., 2010), the main problem in these approaches is the time required for graph computation. The fast graph-based method presented in (Garvin et al., 2009) introduces the idea of a multiscale algorithm, showing that the idea of a pyramidal approach, used in several fields, seems effective in this kind of problems.

At the present time, several graph-based approaches to this task can only work off-line, making them not useful for the ophthalmologists in their everyday clinical practice. For the faster and more effective techniques, there is not any quantitative study of the improvements in performance than can be achieved in this problem. Therefore, establishing where the efficiency can be improved in this task is essential and this is what this work aims for, also showing that it is useful not only to reduce the processing time, but also to avoid segmentation mistakes.

The aim of this paper is, therefore, presenting an multiscale approach for the layer segmentation algorithm based on the min-graph-cut. For that purpose, a pyramidal structure is built based on the original OCT image, and after studying the optimal parameters to design it, a study of time and memory efficiency is presented. Different ways to tackle this approach are evaluated too. The layers that have been included in this work are the top boundaries of the Internal Limiting Membrane (ILM) and bottom boundary of the

González A., Ortigueira C., Ortega M. and G. Penedo M..
Quantitative Study on a Multiscale Approach for OCT Retinal Layer Segmentation.
DOI: 10.5220/0004925107150723
In *Proceedings of the 6th International Conference on Agents and Artificial Intelligence* (ICAART-2014), pages 715-723
ISBN: 978-989-758-015-4

Retinal Pigment Epithelium (RPE). In the text that follows, these layers will be referenced as layers 1 and 6. These layers have been chosen because they are the first to be segmented in several automatic methods applied on the retinal images, because they are which delimit the main part of the retina. In addition, they present different characteristics: the first one is evidently visible in the images, while the second one presents more difficulties, given that the separation between the RPE and the choroid is not always clear, besides the ruptures or discontinuities that can be found on the RPE. The approach presented in this work can be adapted to segment the rest of the layers of the retina.

This paper is organized as follows: In section 2, a review of the graph-based segmentation is presented and section 3 introduces the multiscale (or pyramidal) approach. In section 4 experimental results are shown, with a deep study in the configuration which optimizes the levels in the pyramidal approach and, finally, section 5 offers conclusions and future work.

2 GRAPH-BASED LAYER SEGMENTATION

Graph-based approach transforms the problem of segmentation into that of finding the minimum closed set in a geometric graph. This graph satisfies some smoothness and interaction constraints. The idea is mapping each pixel in the image to a node in the graph. The graph search is guided by some cost functions extracted from the image in order to find its minimum cut. The cost value is assigned to each node, provided by the cost functions designed previously and applied to the image. Therefore, nodes that determine the minimum cut in the graph will correspond to pixels in the image that are interesting to be found; in this case, those corresponding to the layer that is being searched.

As a synthesis of this methodology, Figure 1 shows the phases required to tackle the segmentation of generic a layer: Firstly, a preprocessing to enhance and prepare the image (original images are bounded by black square that must be automatically excluded); after that, the segmentation itself, based on the graph searching exposed before and finally, the representation of the layer over the image.

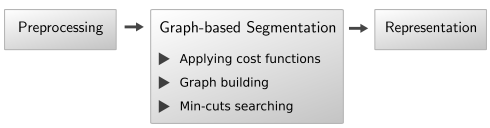

Figure 1: Main phases of the graph-based methodology.

It is necessary to consider that sometimes, the information that can be extracted from the image is not enough, so adding information from adjacent images in an OCT sequence could improve the performance of the method. This is possible because the graph can be designed to perform a 2-D or 3-D geometric searching. Thus, in the 3-D approach, a layer is segmented in an image considering not only values from cost functions applied to it, but also the cost values from the adjacent images in the OCT sequence. This capability is useful in the case that the layer presents discontinuities or low definition in the image. Although the 3-D model seems to be the best approach in the case of sequences of OCT images (always considering an appropriate number of images per sequence), the main problem is the time required for computation in the graph search. The pyramidal structure can be also built in these situations in order to reduce it.

Regarding the phases in the methodology, the multiscale approach involves modifications in the segmentation stage. As it was exposed, information extracted by the cost functions is used to guide the graph searching. Therefore, these functions must be suitably designed to reflect relevant information, in this case, edges location and intensity distribution in the image. In this work, not only cost functions from (Haeker et al., 2007) and (González et al., 2013) are included, but also additional terms that are needed in some levels of the pyramid, as Section 3.2 presents. Synthetically, the cost functions considered are the following:

Edge-based functions, obtained using Sobel operator with a previous Gaussian filtering and a non-maximum suppression, to extract dark-to-light (f_{edge}) and bright-to-dark ($f_{edge}{}'$) transitions. Gradient distance f_g is also considered, taking a distance f_d as value between adjacent pixels. Terms f_α and f_β select the first and last edge in the image, respectively, using thresholds t_α and t_β, whose definition is extended in this work, to consider limits $t_{\beta_{min}}$ and $t_{\beta_{max}}$. Term f_γ erase very close edges in the same column with different direction, while f_Z erase those with the same one. A new term f_X is added in this paper, penalizing the first edge on the image (useful for layer 6 detection).

Intensity-based functions: f_δ and f_ε encourage pixels with bright areas above and below, respectively. Term f_ζ uses similar information to f_δ but encouraging regions on the bottom part of the image. In order to consider dark areas above instead of bright ones, f_ζ' is used.

3 PYRAMIDAL APPROACH

As it was introduced before, the aim of this work is presenting a deep study of a multiscale approach for the graph-based segmentation algorithm, with the purpose of reducing the computation requirements in terms of time and memory. It is based on building a pyramid for each OCT image, where its levels are smaller versions of the original image. The main idea is that the layer segmented in lower resolution images is used in the original one to reduce the area of searching of the graph-based algorithm. Improvement is mainly given by the fact that, for smaller images, smaller graphs are generated to apply the minimum cut algorithm and as the problem in a single-scale has not a linear complexity, linear changes in its dimensions (image size, and therefore, graph size) provide even bigger changes in performance.

In this context, the pyramid is a hierarchical structure consisting of the images resulting of applying certain functions on the original one, whose dimensions are reduced with each transformation. The original (and larger) image is the base of the pyramid, and the successive levels are the resulting images of these transformations. Thus, pyramidal basis conforms the level $i = 0$, whereas the peak corresponds to the level $i = h - 1$, with h the pyramid height.

The construction of this pyramidal structure is the first step in this method and it can be considered as an ascent over the pyramid. Once the original image size has been reduced, according to certain scale factor *sc*, and the different levels of the pyramid have been built, it is possible to descend it. In this descending process, the layer detected in the level above is used in the current level to bound the area of searching, so the graph-based method is applied in a smaller image. Both ascending and descending processes involved in the pyramidal approach are reflected in Figure 2.

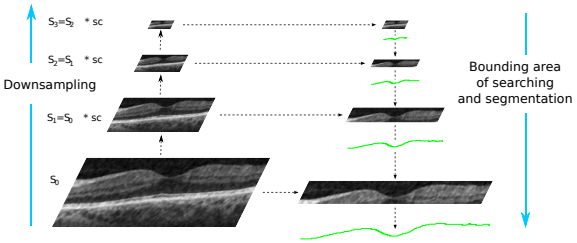

Figure 2: Schema for pyramidal algorithm. At each level i, image size S_i is obtained applying the scale factor *sc* to its dimensions in level $i - 1$.

3.1 The Pyramidal Ascent

The loss of information caused by the resolution reduction must be considered in the ascending process, because at the time that pyramidal height increases, it is more accused. Therefore, it determines the pyramidal height, since the location of the layers becomes more difficult as the structure is ascent. Even though a precise segmentation in the middle levels is not needed, information in the image should be enough to obtain an appropriate detection.

In order to minimize the loss of information, the transformation applied to the images to generate the upper level includes not only a sub-sampling, but also a previous low-pass filtering, making possible that each pixel in the reduced image is influenced by the information of its neighbors. Difference between results obtained with this process and only subsampling are presented in Figure 3.

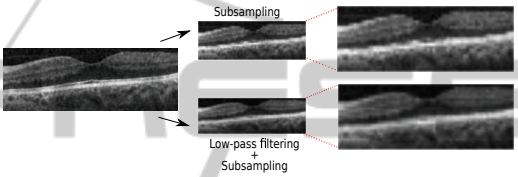

Figure 3: Image obtained during an ascent step using only a sub sampling process and that with a previous low-pass filtering. Zoom has been applied to make the difference more appreciable.

3.2 The Pyramidal Descent

Regarding the descending stage, two basic tasks are needed in each level of the pyramid: firstly, the area of searching is delimited in the current image using the segmentation obtained in the level immediately above (the image is cut and a mask is built based on that, considering flexibility thresholds t_{sup} and t_{inf}), allowing to exclude irrelevant areas in the OCT image. Then, the graph-based method is applied to segment the layer in this level. As the area of interest has been reduced, the number of nodes in the graph is now lower and, therefore, computing time too. The process is reflected in Figure 4.

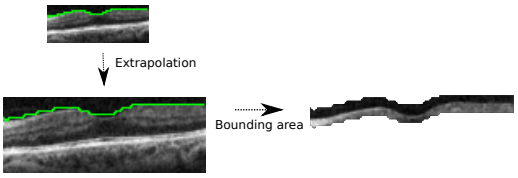

Figure 4: Bounding the area of searching: Layer 1 detected in the image immediately above is extrapolated to the image in the current level and the area of searching is bound.

Once the area of searching is determined and the cost functions have been applied, the graph-based algorithm is used to detect the layer of interest. This entire process is repeated from the peak of the pyramid (where the area of searching is the whole image,

with reduced dimensions) to its base, where the final layer is detected in the original OCT image.

When using a 3-D model, the process is analogous: pyramid is built with 3-D OCT images, and the layer is detected in all of them during the descent stage. In the base of the structure, only the layer segmented in the central image of the group is preserved, since it has the contribution of its adjacent images.

4 RESULTS AND DISCUSSION

Different experiments have been designed in order to find the best pyramidal structures for the segmentation of first and sixth layers and compare its results with those obtain with the original graph-based segmentation method. The data set used in the experiments is composed by 18 OCT sequences, including both healthy and diabetic retinopathy patients. Each sequence consists of 128 images, which makes a total of 2304 images.

These images were captured using Cirrus HD-OCT, with Spectral Domain Technology (Zeiss), at a resolution of 334x334 pixels. All the results have been obtained using an Intel Core TM 2 Duo processor (2,4 GHz) and a RAM of 2 GB.

Three experiments have been designed for each layer separately, since their detection is independent. The first one has the purpose of studying the pyramidal height, in order to determine the number of levels that achieves a successful segmentation with minimum cost. In the second experiment, the feasibility of a descending method without intermediate levels is studied, avoiding the segmentation in certain levels of the structure with the aim of optimizing even more the pyramidal process. Finally, in the last experiment, results of the best pyramids obtained previously are compared with those provided by the original segmentation method.

Given that the aim of this work is optimizing the efficiency of the graph-based segmentation method, maintaining the accuracy in the segmentation results is essential. With that purpose, experiments 1 and 2 are done in two steps: firstly the feasible pyramidal heights are studied, in order to consider pyramids with enough number of levels (but not excessive) to achieve appropriate segmentation results. After that, efficiency is studied for those structures. Thus, at each experiment, both effectiveness (successful segmentation) and efficiency (in terms of consumed time and memory) are considered.

It is necessary to take into account that, in these experiments, layer 1 is segmented using a 2-D graph, since its location is evident in the images, and the information from adjacent images is not needed. Regarding layer 6, a 3-D graph is needed, due to the discontinuities in this layer, in addition to the fact that the borderline between RPE and Choroids is not well defined in the images. The 3-D graph for layer 6 is built with overlapping groups of 3 consecutive images.

Parameters involved in the methodology have been extracted empirically. The factor scale sc used in this work is set to 0.5, so dimensions for the image located in the level i of the pyramid are the half of the image immediately below (level $i-1$).

4.1 Experiment 1: Determining the Optimal Pyramid Height

In this set of experiments, pyramids of different height are evaluated, in order to determine the number of levels that allows to obtain a successful segmentation of each layer with minimum computational cost. This task is done in two steps: firstly, a coarse study of the heights than be considered to built pyramids for both layers is done. After that, time and memory required by the pyramid-based approach using these heights to detect layers 1 and 6 is deeply studied.

Regarding layer 1, preliminary experiments show that segmentation does not present mistakes for pyramids of up to 4 levels, whereas layer 6 can not be correctly segmented with structures higher than 3 levels. Once that the maximum number of levels for each pyramid is known, performance is studied to select the most appropriate structure. Table 1 shows results obtained, while Figure 5 reflects them graphically.

Table 1: Time and memory consumed in the segmentation task using pyramids of different heights, both expressed as mean (standard deviation). Best time results have been highlighted.

		$h=2$	$h=3$	$h=4$
Layer 1	Time (s)	58.44 (12.88)	30.22 (6.03)	**29.67 (5.57)**
	Memory (MB)	103.22 (1.56)	103.83 (1.86)	104.00 (1.88)
Layer 6	Time (s)	1216.94 (557.36)	**562.17 (93.10)**	–
	Memory (MB)	115.11 (4.79)	123.22 (4.87)	–

4.1.1 Discussion

First aspect to be observed is that the consumed memory does not change significantly using different levels in the pyramid, so it is not a decisive factor in the selection of the best structure. However, it is observed that layer 6 requires more memory than the layer 1. Obviously, this is because of the 3-D model used to detect that layer.

The number of levels has more evident repercussions in the computation time. As Figure 5 (a) exposes, time required to detect layer 1 decreases considerably when $h = 3$, whereas the small difference

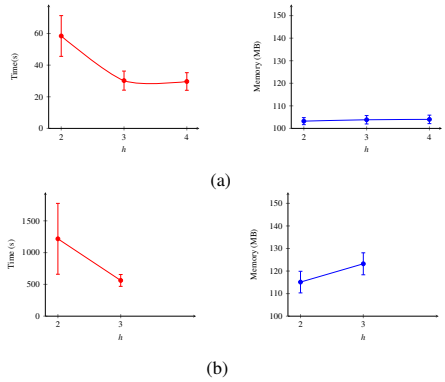

Figure 5: Time and memory consumed using pyramids of different heights to segment layer 1 (a) and 6 (b).

in performance with $h = 3$ and $h = 4$ indicates that this extra level does not provide relevant information to bound the area of searching in the lower levels. This is due to the fact that some margins are needed in the processes of cutting and mask extraction. Therefore, although segmentation with higher pyramids may be possible, their contribution to reduce computation time is not relevant.

Time consumed to detect layer 6, shown in Figure 5(b), also experiments an evident decreasing when the number of levels increases. In addition, it is observed that improvement using $h = 3$ regarding $h = 2$ is higher than the obtained for layer 1. This is caused by the 3-D model used to detect layer 6, which is more sensitive to the different sizes of the image (and consequently, the associated graph) than a 2-D model. In a intuitive way, the number of arcs between nodes is higher in the 3-D model, making the searching harder. Therefore, when they are reduced, computation time changes in a more accused way.

With regards to the standard deviation in the presented measures, it is remarkable that the variability is mainly caused by the operations performed in the preprocessing stage of the methodology. In this first phase, the dimensions of the input OCT image are optimized, removing the dark top and bottom, which do not provide useful information. The different shape of the retinal structure in the OCT images of the validation set causes a variation in the size of the input image for the segmentation stage, which thereby require different execution times. Results, however, show that standard deviation does not affect in a significant way to the efficiency, compared to the other factors do.

4.2 Experiment 2: Optimizing the Pyramidal Descent

Previous experiments have determined the optimal height for the pyramidal structure for both layers 1 and 6. Thus, after optimizing the process of ascending the pyramid, an improvement in the descent can be suggested, studying if the levels between the peak of the pyramid and its base are needed or instead, the application of the algorithm in all of them can be avoided, as depicted in Figure 6. This method will be referenced as *direct descent*, because it intends to extrapolate directly the layer segmented in the peak of the pyramid to the image in its base, instead of exploring all the levels to bound the area of searching at each one. Thus, the min-cut searching is only applied in these two levels.

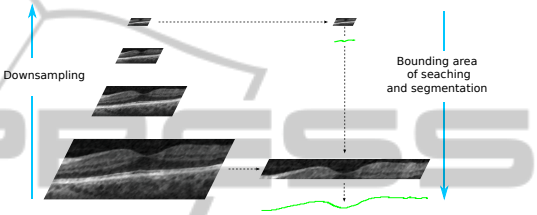

Figure 6: Schema for the pyramidal-based algorithm, including the *direct descent* method.

This experiment is developed following an analogous scheme to the previous one: firstly, the optimal height for the pyramids is studied and then, the performance for each possible structure is evaluated. Preliminary results show that an appropriate segmentation of layer 1 with structures with height h more than 3 is not possible, so results for the feasible structures are presented in Table 2 and Figure 7. Computation times required in this experiment are also compared with those obtained in the previous one (Figure 8), because determining if the *direct descent* is possible is not enough, but also if it provides an improvement with regards to the best performance obtained in the previous set of experiments.

Table 2: Time and memory consumed in the segmentation task using the *direct descent*, both expressed as mean (standard deviation). Best time results have been highlighted.

		$h = 2$	$h = 3$
Layer 1	Time (s)	58.44 (12.88)	**26.78 (5.00)**
	Memory (MB)	103.22 (1.56)	104.22 (1.66)
Layer 6	Time (s)	**1216.94 (557.36)**	2988.17 (336.62)
	Memory (MB)	115.11 (4.79)	129.89 (3.74)

4.2.1 Discussion

In contraposition to results obtained in the previous experiment, in this case, a suitable segmentation of layer 1 can not be obtained using structures higher that $h = 3$. This is due to the detection mistakes present in the top of the pyramid caused by the loss of information inherent to the downsampling. In the ori-

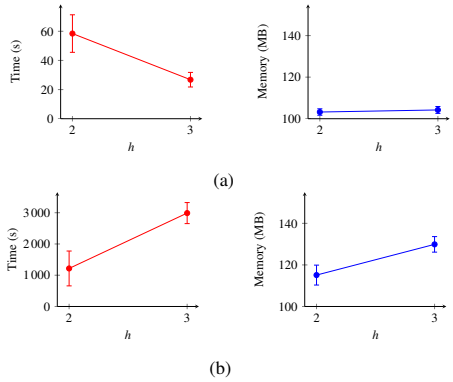

Figure 7: Time and memory consumed using the *direct descent* method to segment layer 1 (a) and 6 (b).

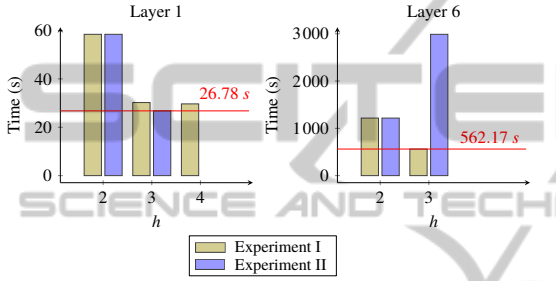

Figure 8: Comparison in time between both experiments to segment layer 1 and layer 6.

ginal descending method, these deficiencies are corrected gradually at each level, so the area of searching in the base is the appropriate. In the *direct descent* proposed in this experiment, these small errors at the peak of the structure are transferred directly to its base, and also magnified due to the larger scale of extrapolation.

Results show that, for layer 1, consumed memory is approximately stable, whereas for layer 6 slightly increases, mainly due to the larger areas of searching required by this layer, given the difficulties to determine its precise location. However, it is not a critical factor in the selection of one or another method. Regarding execution time, it is observed that, while using the *direct descend* method involves an improvement to segment layer 1, it does not to layer 6. Once again, this is related to the larger areas of searching used to detect this layer. Thus, it is possible to affirm that the middle levels in the pyramidal structure are not essential for layer 1, but they are needed for layer 6.

Having analyzed the performance of the pyramidal structures with the *direct descent* approach, a comparison between these results and those obtained Experiment 1 is necessary. Since consumed memory remains fairly stable, execution time comparison (Figure 8) determines the best structure and the method used to descend it for each layer.

As it was explained before, the information available in the peak of the pyramid with $h = 3$ is enough to avoid using the intermediate levels in the segmentation of layer 1. On the other hand, detecting layer 6 with the *direct descent* method is not profitable in terms of performance, because of the complex location of this layer. Not considering the information of the intermediate levels to correct the deficiencies of the segmentation in the peak of the structure involves using a larger area of searching in the basis. Therefore, computation time increases, specially using a 3-D model. Thus, unlike layer 1, the best approach to detect layer 6 consist in applying the algorithm in all the levels of the structure, as it was presented in Experiment 1.

4.3 Experiment 3: Comparison with the Single-scale Approach

Experiments exposed previously have provided the best configurations for the pyramidal approach proposed to detect layers 1 and 6. Now, a comparison between original single-scale approach and the new pyramidal multiscale one is presented, considering not only terms of performance but also effectiveness (accuracy in the segmentation obtained).

Table 3 shows performance results obtained for both options (results presented for the pyramid-based method are those obtained with the best structures analyzed the previous experiments). With regards to the segmentation accuracy, most test show that both approaches provide similar results (some samples obtained with each method are presented in Figure 9). The most interesting fact is that multiscale approach solves some mistakes made by the single-scale method, as Figure 10 shows, although this will be commented in detail in the discussion.

Table 3: Consumed time and memory comparison between the simple-scale method and the pyramidal-approach. Results are expressed as: mean (standard deviation). Percent of improvement in time has been highlighted.

		Original Method	Pyramidal Approach	Improvement(%)
Layer 1	Time (s)	1795.28 (873.55)	26.78 (5.00)	**98.51**
	Memory (MB)	148.61 (11.71)	104.22 (1.66)	29.87
Layer 6	Time (s)	24499.39 (13259.34)	562.17 (93.10)	**97.71**
	Memory (MB)	162.78 (6.31)	123.22 (4.87)	24.30

4.3.1 Discussion

Figure 9 shows that the quality obtained with the single-scale method is maintained with the proposed multiscale approach. Despite the similarity between both segmentations, there are situations in which the

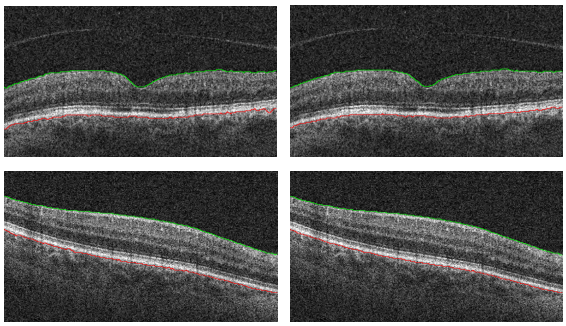

(a) (b)

Figure 9: Segmentation samples obtained for layer 1, in green, and 6, in red: (a) single-scale method; (b) pyramidal approach.

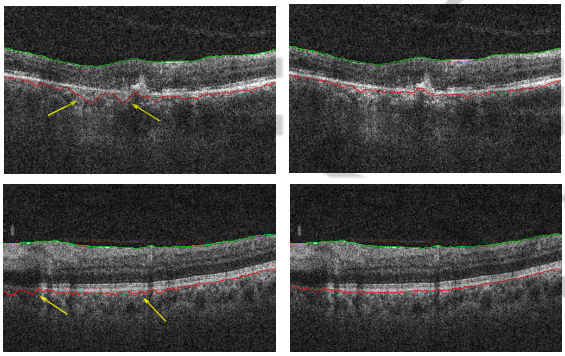

(a) (b)

Figure 10: Segmentation results obtained for layer 1 and 6: (a) single-scale method; (b) pyramidal approach. Yellow arrows indicate the mistakes using the single-scale method, which are avoided using the pyramidal structure.

pyramid-based method provides better results. Thus, it is possible to affirm that the loss of information inherent to the pyramidal process and the downsampling, as well as the bounded area of searching obtained, are really relevant. In particular, these terms allow correcting some mistakes caused by the information present in the original image. This is specially remarkable in the case of layer 6, given that the choroid, located below it and with similar properties, can involve wrong segmentation in some parts of the image. As samples in Figure 10 show, these errors are not made using the pyramidal approach.

On the other hand, comparison between both solutions in terms of performance presented in Table 3 show that, as it was mentioned before, the most significant factor to take into account is the computation time. It is remarkable that a relevant leap in time is done (even in magnitude order, considering terms of hours in the single-scale problem to minutes and seconds in the multiscale approach).

Results show the high computation time required by the single-scale method, which make it nonviable, specially for layer 6 detection (mean time required over six hours). Proposed optimization, with configurations for pyramidal structures exposed in the previous experiments, achieves a significant improvement in time for each layer over the 97%. Additionally, although consumed memory is not excessive in any of the approaches, pyramid-based solution reduces it in more than a 20% in each layer. For layer 1, segmentation using three-level pyramidal structure and the *direct descend* from the peak to the base is 67 times faster than the original procedure, as Table 3 presents. However, the improvement is lower for layer 6, whose proposed approach is 43 times lower than the original. This difference is mainly caused by the higher difficulty in the location of this layer, as well as the use of 3-D model, as it was introduced in the previous experiments.

Pyramid-based approach also involves an improvement in the variability of the consumed time. For instance, results in Table 3 show that segmentation of layer 1 with the original method can vary in function of the patient until a 48% of the mean time (approximately 14 minutes), whereas the pyramidal method presents a dispersion of 18.6% with respect to the mean value (5 seconds). Regarding layer 6, reduction is analogous.

This improvement in the standard deviation is mainly provided by the bounding area process (Section 3.2), which has a direct repercussion in the graph size generated in the detection. In this step, cutting process affects mainly to the number of rows in the image located on the pyramidal peak (lower levels use a mask to bound even more the area of interest). In addition, segmentation process in the peak of the pyramid barely affects in the global time required to detect a layer. Therefore, as variability between patients is caused by the cutting in the descent stage and it affects specially to the image on the highest level in the pyramid (whose segmentation time is short), it seems obvious that the influence in the total time will be also small. In contraposition to that, in the original methodology the difference in size between two images has a more relevant repercussion, because the number of nodes (and therefore, the number of arcs) erased in the cutting is much higher than that done in the peak of a pyramid. Therefore, changes in terms of dispersion are which should be expected and, as it was determined in Experiment 1, this difference is not a significant factor to take into account.

As a synthesis of the results obtained in this experiment, it is shown that the pyramid-based approach provides better results than the single-scale method in terms of computation time, at the time that maintains, and also improves, segmentation obtained with this

Table 4: Parameters used to segment layer 1. They correspond to the best configuration obtained after the experiments (three-level pyramid, with the *direct descent* method).

Level (i)	Parameter												
	f_1	w_{edge}	w_g	w_α	w_β	w_γ	$w_{\zeta'}$	f_d	t_α	$t_{\beta_{min}}$	$t_{\beta_{max}}$	t_{sup}	t_{inf}
2	$f_{edge}+f_g+f_\alpha+f_\beta+f_{\zeta'_N}$	1000	2000	1000	1000	-	1000	20	5	0	2	-	-
0	$f_{edge}+f_g+f_\alpha+f_\gamma$	1000	2000	1000	-	1000	-	20	10	2	10	15	10

Table 5: Parameters used to segment layer 6. They correspond to the best configuration obtained after the experiments (three-level pyramid, with the original descent method).

Level (i)	Parameter												
	f_6	$w_{edge'}$	w_g	w_δ	w_ε	$w_{\zeta'}$	w_X	f_d	ws_δ	ws_ε	t_X	t_{sup}	t_{inf}
2	$f_{edge'}+f_g+f_\delta+f_X$	1000	2000	1000	-	-	1000	20	1	-	5	-	-
1	$f_{edge'}+f_g+f_\delta+f_\varepsilon+f_{\zeta'_N}+f_X$	2000	2000	2000	1500	1000	1000	20	1	1	5	15	5
0	$f_{edge'}+f_g+f_\delta+f_\varepsilon+f_{\zeta'}$	2000	2000	1500	1000	1000	-	20	1	1	-	7	7

method.

5 CONCLUSIONS AND FUTURE WORK

This paper presents a study of a multiscale approach for a graph-based method to segment retinal layers in OCT images. This approach is evaluated on two retinal layers, considering terms of computing time and memory. Three experiments have been designed to evaluate the different configurations that can be taken into account in this problem, in order to achieve the most successful results. Values for parameters in the graph-based method are presented in Tables 4 and 5, corresponding to the best configuration obtained in the experiments. Quantitative measures show that this approach improves considerably the performance of the original method. They also determines the method that should be applied in each layer during the pyramidal descent. Accuracy has been evaluated too, because segmentation results obtained by the single-scale method must be maintained. This approach achieves not only the same results, but also improve them, obtaining successful segmentation in situations where the single-scale method makes mistakes.

ACKNOWLEDGEMENTS

This paper has been partly funded by the Ministerio de Ciencia e Innovación under TIN2011-25476 project of the Spanish Government (A. Gonzalez acknowledges the support of Secretaría de Estado under *FPI* Grant Program).

REFERENCES

Albrecht, P., Ringelstein, M., Mueller, A., Keser, N., Dietlein, T., Lappas, A., Foerster, A., Hartung, H., Aktas, O., and Methner, A. (2012). Degeneration of retinal layers in multiple sclerosis subtypes quantified by optical coherence tomography. *Multiple Sclerosis Journal*.

Bowd, C., Weinreb, R., Williams, J., and Zangwill, L. (2000). The retinal nerve fiber layer thickness in ocular hypertensive, normal, and glaucomatous eyes with optical coherence tomography. *Archives of Ophthalmology*, 118(1):22–26.

Chiu, S. J., Li, X. T., Nicholas, P., Toth, C. A., Izatt, J. A., and Farsiu, S. (2010). Automatic segmentation of seven retinal layers in sdoct images congruent with expert manual segmentation. *Optics Express*, 18(18):19413–19428.

Garvin, M. K., Abràmoff, M. D., Wu, X., Russell, S. R., Burns, T. L., and Sonka, M. (2009). Automated 3-d intraretinal layer segmentation of macular spectral-domain optical coherence tomography images. *IEEE Trans. Med. Imaging*, 28(9):1436–1447.

González, A., Penedo, M. G., Vázquez, S. G., Novo, J., and Charlón, P. (2013). Cost function selection for a graph-based segmentation in OCT retinal images. In *LNCS: Computer Aided Systems Theory, Revised Selected Papers EUROCAST 2013*.

Haeker, M., Sonka, M., Kardonc, R., Shah, V. A., Wu, X., and Abrmoff, M. D. (2007). Automated segmentation of intraretinal layers from macular optical coherence tomography images. *Proc. SPIE: Medical Imaging*, 6512.

Keane, P. A., Patel, P. J., Liakopoulos, S., Heussen, F. M., Sadda, S. R., and Tufail, A. (2012). Evaluation of age-related macular degeneration with optical coherence tomography. *Survey of Ophthalmology*, 57(5):389–414.

Puzyeyeva, O., Lam, W. C., and Flanagan, J. e. a. (2011). High-resolution optical coherence tomography retinal

imaging: A case series illustrating potential and limitations. *J. Ophthalmology*.

Sánchez-Tocino, H., Álvarez-Vidal, A., Maldonado, M. J., Moreno-Montañes, J., and García-Layana, A. (2002). Retinal thickness study with optical coherence tomography in patients with diabetes. *Investigative Ophthalmology & Visual Science*, 43(5):1588–94.